A model of total swimming costs in turbulent flow for juvenile Atlantic salmon (*Salmo salar*)[1]

Eva C. Enders, Daniel Boisclair, and André G. Roy

Abstract: Juvenile Atlantic salmon (*Salmo salar*) live in rivers characterized by highly turbulent flows. In these environments, flow turbulence is associated with a wide range of instantaneous flow velocities, which may affect the energetic costs of habitat utilization of juvenile Atlantic salmon. The purpose of our work was to develop a swimming costs model for juvenile Atlantic salmon that especially accounts for the effects of velocity fluctuations in turbulent environments. We estimated the total swimming costs of fish in a respirometer in which we produced five turbulent flow conditions, each characterized by a mean and a standard deviation of flow. Respirometry experiments were conducted at water temperatures of 10, 15, and 20 °C with fish ranging in size between 4.3 and 17.6 g at three mean flow velocities (18, 23, and 40 $cm \cdot s^{-1}$) and three standard deviations of flow velocity (5, 8, and 10 $cm \cdot s^{-1}$). Our results confirmed that total swimming costs increased with an increase of water temperature, body mass, mean flow velocity, and standard deviation of flow velocity ($R^2 = 0.93$). Water temperature, body mass, mean flow velocity, and standard deviation of flow velocity contributed respectively 2%, 31%, 46%, and 14% to the explained variation in total swimming costs.

Résumé : Les juvéniles du saumon atlantique (*Salmo salar*) vivent dans les rivières caractérisées par des écoulements fortement turbulents. Dans ces environnements, la turbulence de l'écoulement est associée à un vaste étendu des vitesses instantanées, ces dernières pourraient affecter les coûts énergétiques des juvéniles du saumon atlantique lors de l'utilisation de l'habitat. Le but de notre travail était de développer un modèle de coût de nage des juvéniles du saumon atlantique qui tient spécialement compte des effets des fluctuations de vitesse dans un environnement turbulent. Nous avons estimé les coûts totaux de nage de poisson dans un respiromètre dans lequel nous avons produit cinq conditions turbulentes, chacune caractérisée par une moyenne et un écart-type distincts de la vitesse de l'écoulement. Les expériences respirométriques ont été réalisées à 10, 15 et 20 °C en utilisant des poissons d'une taille variant de 4,3 à 17,6 g, à trois vitesses moyennes (18, 23 et 40 $cm \cdot s^{-1}$) et à trois écart-types de vitesse (5, 8 et 10 $cm \cdot s^{-1}$). Nos résultats confirment que les coûts totaux de nage augmentent avec une augmentation de la température de l'eau, de la masse corporelle, de la vitesse moyenne et de l'écart-type de vitesse ($R^2 = 0{,}93$). La température de l'eau, la masse corporelle, la vitesse moyenne et l'écart-type de vitesse contribuent respectivement pour 2, 31, 46 et 14 % de la variation expliquée dans les coûts totaux de nage.

Introduction

Bioenergetics models may be applied to assess fish habitat quality and spatial distribution (Fausch 1984; Nislow et al. 2000). In a habitat with favorable growth conditions, fish obtain a positive balance between the energetic gains through food consumption, the energetic costs for metabolism, and the losses from excretion and egestion (Fausch 1984; Hill and Grossman 1993). Increased growth may lead to fitness advantages with respect to foraging abilities and competitive capacities (Hill and Grossman 1993; Cutts et al. 1998), overwinter survival (Cunjak and Therrien 1998; Morgan et al. 2000), and age of first reproduction (Hutchings and Jones 1998; Morgan et al. 2002). However, the precision of the predictions of bioenergetics models depends on the reliability of the submodels used to estimate the different components of fish energy budget (Hansen et al. 1993; Ney 1993). Activity metabolism may represent up to 40% of the energy budget (Brett and Groves 1979; Boisclair and Leggett 1989). Consequently, the precise quantification of the activity me-

Received 5 April 2004. Accepted 17 December 2004. Published on the NRC Research Press Web site at http://cjfas.nrc.ca on 26 May 2005.
J18061

E.C. Enders[2,3] and D. Boisclair. Département de sciences biologiques, Université de Montréal, C.P. 6128, Succursale Centre-ville, Montréal, QC H3C 3J7, Canada.
A.G. Roy. Département de géographie, Université de Montréal, C.P. 6128, Succursale Centre-ville, Montréal, QC H3C 3J7, Canada.

[1]Contribution to the program of CIRSA (Centre Interuniversitaire de Recherche sur le Saumon Atlantique).
[2]Corresponding author (e-mail: enderse@dfo-mpo.gc.ca).
[3]Present address: Fisheries and Oceans Canada, Ecological Sciences Section, 80 East White Hills Road, P.O. Box 5667, St. John's, NL A1C 5X1, Canada.

 doi: 10.1139/F05-007

tabolism is of great interest to obtain appropriate predictions from bioenergetics models (Boisclair and Leggett 1989; Hansen et al. 1993; Ney 1993).

Estimation of the activity metabolism requires the description of the movements performed by the fish in their natural environment (i.e., number, duration, and speed of movements) and the quantification of the energetic costs of performing these movements. Generally, the energy expenditures associated with the movements of stream-dwelling fish are estimated by models derived from respirometry experiments with fish swimming at a steady speed in a flume designed to minimize flow heterogeneity (Brett 1964; Beamish 1978). However, in their natural environment, stream-dwelling fish are often confronted with a highly turbulent flow that may affect their activity metabolism. For instance, Pavlov et al. (2000) have shown that the sustained swimming speed and the critical swimming speed of gudgeon (*Gobio gobio*) and roach (*Rutilus rutilus*) decrease with an increase of turbulence intensity (standard deviation/mean flow velocity). This suggests that the activity metabolism increases with an increase of turbulent intensity (Pavlov et al. 2000). In contrast, Liao et al. (2003) demonstrated that adult rainbow trout (*Oncorhynchus mykiss*) swimming behind an obstacle producing a regular vortex shedding use the energy of these vortices to maintain their position in turbulent flows while reducing their muscle activity. This indicates that activity metabolism of fish using vortices that occur in turbulent flows may be lower than in the absence of such vortices. However, in natural gravel-bed rivers, vortex shedding may be more dynamic and more variable in location, occurrence, and intensity than under a controlled laboratory situation. Therefore, it may be more difficult for stream-dwelling fish to benefit from vortices in natural flow environments. Furthermore, in natural gravel-bed rivers, we also observe large-scale flow structures that extend over the entire water column. They may be seen as a temporal succession of quasi-periodic pulses of high- and low-speed fluid lasting several seconds (Roy and Buffin-Bélanger 2001; Roy et al. 2004). The high-speed pulses are generally directed towards the river bed whereas the low-speed pulses develop towards the water surface. Measurements of these turbulent flow structures suggest that the flow velocity can change three- to eightfold relative to the mean flow velocity within 1–5 s (Roy et al. 1999). These large-scale flow structures vary in length between three and five times the water depth (Roy et al. 2004). Fish are confronted by these flow fluctuations, and in a preliminary study, we showed that the cost of swimming in such a temporally fluctuating flow may be two to four times the values predicted by steady-swimming models (Enders et al. 2003). However, the energetic cost of swimming under turbulent flow conditions was estimated using only a single water temperature and fish body mass. In the present study, we conducted experiments under a wider range of water temperature, body mass, mean flow velocity, and turbulent conditions.

The objectives of this study were to (*i*) evaluate the effect of fish body mass, water temperature, mean flow velocity, and descriptors of flow turbulence on the energetic cost of swimming in fish, (*ii*) develop swimming costs models for fish swimming under turbulent flow conditions, (*iii*) assess the relative power of different descriptors of flow turbulence in predicting total swimming costs, and (*iv*) compare the prediction of turbulent swimming models with existing forced-swimming models over a range of abiotic conditions.

Material and methods

We attained our objectives by performing a total of 104 respirometry experiments during which we subjected individual fish ranging from 4.3 to 17.6 g wet mass to turbulent flow conditions. Respirometry experiments were conducted at 10, 15, and 20 °C. We estimated total swimming costs under four turbulent flow conditions defined by the combination of two means (18 and 23 $cm \cdot s^{-1}$) and two standard deviations (5 and 8 $cm \cdot s^{-1}$) of flow velocity. Eight respirometry experiments, each involving a fish of a different mass, were performed for each combination of water temperature and flow condition (further referred to as suite of experiments). In addition to these 12 suites of experiments (3 water temperatures × 4 flow conditions), we conducted another suite of eight experiments at 15 °C and under a turbulent flow condition characterized by a mean flow velocity of 40 $cm \cdot s^{-1}$ and a standard deviation of flow velocity of 10 $cm \cdot s^{-1}$.

Fish

We evaluated the energetic cost of swimming in a turbulent flow using juvenile Atlantic salmon (*Salmo salar*; ages 1+ and 2+). The body mass (wet) of the juvenile Atlantic salmon (JAS) ranged from 4.3 to 17.6 g. JAS are particularly suitable for this study because their natural habitat comprises riffle sections in gravel-bed rivers that are characterized by a highly turbulent flow. JAS are drift feeders and undertake feeding motions from the riverbed towards the water surface to capture drifting invertebrates (Kalleberg 1958). During these motions, JAS experience rapid changes in flow velocities and structure.

JAS were provided by the Pisciculture de Tadoussac (operated by the Société de la Faune et des Parcs du Québec, Canada). These fish are the offspring from the crossing of wild genitors originating from the Sainte-Marguerite River (Saguenay Region, Quebec, Canada). The juveniles were transferred to the Université de Montréal where they were kept in 500-L Living Stream aquaria (LSW 700) (Frigid Units Inc., Toledo, Ohio). Fish were adapted for a period of 1 month at the targeted water temperatures (10, 15, and 20 °C ± 0.5 °C) before starting a suite of experiments. Fish were fed daily with commercial food pellets (Corey Feed Mills Ltd., Fredericton, New Brunswick).

Respirometry

The details of the experimental design and procedure that we employed are fully described in Enders et al. (2003). They are only summarized here. The respirometer consisted of a Plexiglas© box that could be hermetically sealed. The respirometer contained two pumps (further referred to as pumps 1 and 2) and a bottle-shaped swimming chamber. The narrow neck of the swimming chamber was connected to pump 1 (Jacobs Canada Inc., Mississauga, Ontario) that generated the turbulent flow in the swimming chamber. Pump 2 (Powerhead, Montréal, Quebec) transferred water from the respirometer to an oxygen meter (Intap, model 565) (Mettler

Table 1. Mean flow velocity, standard deviation of the flow velocity, and minimum and maximum values measured for the streamwise (u), vertical (v), and lateral (w) velocity components at five different flow conditions, turbulence intensity (TI; standard deviation (u_{SD})/mean velocity ($\bar{u}$)), and turbulent kinetic energy (TKE).

Velocity vector	Low velocity, low turbulence	Low velocity, medium turbulence	Medium velocity, low turbulence	Medium velocity, medium turbulence	High velocity, high turbulence
$\bar{u}$ (cm·s^{-1})	18.1	18.3	23.1	23.1	40.7
u_{SD} (cm·s^{-1})	5.1	8.2	5.1	8.0	10.3
u_{min} (cm·s^{-1})	3.6	0.5	5.0	0.7	2.5
u_{max} (cm·s^{-1})	34.6	39.7	35.2	43.7	76.6
$\bar{v}$ (cm·s^{-1})	0.1	0.0	0.0	0.0	–2.1
v_{SD} (cm·s^{-1})	4.9	7.0	5.0	7.4	14.8
v_{min} (cm·s^{-1})	–21.9	–24.8	–22.9	–29.9	–74.7
v_{max} (cm·s^{-1})	21.9	23.7	21.5	29.8	51.0
$\bar{w}$ (cm·s^{-1})	0.2	0.1	0.0	0.3	3.1
w_{SD} (cm·s^{-1})	5.5	7.6	5.5	7.5	12.4
w_{min} (cm·s^{-1})	–21.9	–26.0	–27.4	–28.2	–49.4
w_{max} (cm·s^{-1})	23.3	26.6	26.5	30.7	56.0
TI*	0.27	0.44	0.22	0.34	0.25
TKE (g·cm^{-1}·s^{-2})	66.8	139.4	68.8	143.6	416.2

*Unitless.

Toledo, Mississauga, Ontario). The energetic cost of swimming against a turbulent flow was quantified by measuring the oxygen depletion over time with the oxygen meter (±0.01 mg O_2·L^{-1}).

Turbulent flow

The turbulent flow within the swimming chamber was created by modulating the electric current that powered pump 1. The flow in the swimming chamber was quantified using an acoustic Doppler velocimeter (ADV) (Sontek, San Diego, California). The turbulent flow was measured in the absence of the fish to avoid interference caused by its body and movements. The ADV allowed us to record the three orthogonal velocity components of the flow (streamwise (u), vertical (v), and lateral (w)). The instantaneous velocities of the three orthogonal velocity components were measured at a frequency of 25 Hz. The ADV also permitted us to define the settings of the components of the electric current that could create five different flow conditions (Table 1). The flow conditions are characterized by a selected combination of three mean streamwise flow velocities ($\bar{u}$; low flow velocity = 18 cm·s^{-1}, medium flow velocity = 23 cm·s^{-1}, and high flow velocity = 40 cm·s^{-1}) and three standard deviations of the streamwise flow velocity (u_{SD}; low turbulence = 5 cm·s^{-1}, medium turbulence = 8 cm·s^{-1}, and high turbulence = 10 cm·s^{-1}). The settings for the five turbulent flow conditions were selected because they are within the range of mean flow velocities (5–40 cm·s^{-1}) (DeGraaf and Bain 1986; Guay et al. 2000) and of standard deviations of flow velocity (4–14 cm·s^{-1}) observed at the focal point used by JAS under natural conditions (Enders et al. 2005).

Velocity time series were recorded for 5 min at the beginning and end of each suite of respirometry experiments. This strategy was adopted to verify the stability and repeatability of the flow created by our apparatus for given settings of the components of the electric current that powered pump 1. The stability of the five experimental flow conditions was tested using Student's t test. Such t tests were performed to compare the mean streamwise flow velocities recorded before and after a suite of experimental observations. The repeatability of the specific turbulent flow condition produced at different water temperatures was tested using a one-way analysis of variance (ANOVA) comparing the mean streamwise flow velocities. During this analysis, the velocity time series obtained before and after a suite of experimental observations were used as replicates. The stability and repeatability of the standard deviations of the streamwise flow velocities were tested using the Levene's test of the homogeneity of variance using the same procedure.

We obtained the means and standard deviations for the velocity components (u, v, w) for each flow condition. From the means and standard deviations for u, we calculate the turbulence intensity (TI; standard deviation (u_{SD})/mean velocity ($\bar{u}$)). We also used the three velocity components provided by the ADV to calculate the turbulent kinetic energy (TKE) (grams per centimetre per second squared):

$$(1) \qquad \mathrm{TKE} = 1/n \sum_{i=1}^{n} 0.5\rho(u_i'^2 + v_i'^2 + w_i'^2)$$

where n is the number of instantaneous velocity fluctuations (7500 measurements per velocity time series), ρ (grams per cubic centimetre; depending on water temperature used in our experiments) is the water density, and u_i', v_i', and w_i' (centimetres per second) represent the instantaneous velocity fluctuation of the three velocity components.

The five different flow conditions created by our apparatus during the experiments corresponded to the targeted means (18, 23, and 40 cm·s^{-1}) and standard deviations (5, 8, and 10 cm·s^{-1}) of flow velocity. Mean flow velocities were always within 1.8%, 0.4%, and 1.7% of the targeted values for the low, medium, and high flow velocities, respectively (Table 1). The standard deviation of the streamwise flow velocity was 5.1, 8.1, and 10.3 cm·s^{-1} for the low, medium, and

high turbulence condition, respectively, and did not vary by more than 4.3% among experiments. Mean vertical and lateral flow velocities were close to 0 $cm \cdot s^{-1}$ (–2.1 to 3.1 $cm \cdot s^{-1}$). The corresponding standard deviation of the vertical and lateral flow velocity ranged from 4.9 to 14.8 $cm \cdot s^{-1}$. TI of the five different flow conditions varied between 0.22 (medium flow velocity and low turbulence) and 0.44 (low flow velocity and medium turbulence). TKE ranged from 66.8 $g \cdot cm^{-1} \cdot s^{-2}$ (low flow velocity and low turbulence) to 416.2 $g \cdot cm^{-1} \cdot s^{-2}$ (high flow velocity and high turbulence) (Table 1).

For any given flow condition, $\bar{u}$ and u_{SD} did not vary significantly among the recordings performed before and after a suite of experimental observations (stability test for $\bar{u}$: $0.42 < p < 0.98$, variation = 0.0%–0.3%; stability test for u_{SD}: $0.12 < p < 0.94$, variation = 0.2%–2.1%). Similarly, the characteristics of specific flow conditions produced at different water temperatures did not vary significantly among experiments (stability test for $\bar{u}$: $0.39 < p < 0.99$, variation = 0.1%–0.9%; stability test for u_{SD}: $0.17 < p < 0.69$, variation = 0.1%–2.3%). These results suggest that the flows created by our apparatus were stable and repeatable.

Total swimming costs

A single fish was selected at random from our stock of experimental fish, kept separately, and not fed for 2 days before the experiment to avoid increased metabolic rates due to digestion (Brett and Groves 1979). The fish was introduced into the swimming chamber 24 h before the beginning of the experiment to allow it to adapt to the experimental conditions. The initial oxygen concentration was measured at the beginning of the experiment and subsequently at every 30 min until the end of an experiment. We monitored fish behavior during each experiment using a web cam (Sony Electronics Inc., Oradell, New Jersey) to ensure that fish were continuously swimming. An experiment ended after 6 h for the low and medium flow velocity experiments and after 3 h for the high flow velocity experiments. No observation was made below 7.6 mg $O_2 \cdot L^{-1}$ to minimize the influence of low oxygen concentration on the fish behavior (Beamish 1978). At the end of an experiment, the fish was removed from the respirometer, anaesthetized (clove oil, 0.6 $mg \cdot L^{-1}$), weighed (grams wet), and measured (total body length, centimetres). The biological oxygen demand (BOD) was determined within 3 h of an experiment using the same procedure but without fish. We estimated the total oxygen consumption rate (sum of standard metabolic rate plus net swimming costs) of fish (V_{O_2}) (milligrams of oxygen per hour) as

$$(2) \qquad V_{O_2} = \Delta O_2 / \Delta t V_w - \mathrm{BOD}$$

where ΔO_2 is the difference in oxygen concentration between two consecutive oxygen concentration measurements (milligrams of oxygen per litre), Δt is the time interval of 0.5 h between two consecutive oxygen concentration measurements, V_W (litres) is the volume of water in the respirometer excluding the solid volume of pumps, swimming chamber, and fish, and BOD is the biological oxygen demand by microorganisms in the water (milligrams of oxygen per hour). The BOD was always below the detection limit of the oxygen sensor. As we measured oxygen concentration within the swimming chamber at 30-min intervals over 3 or 6 h, we obtained 6 or 12 V_{O_2} values per experiment, respectively. We then calculated the mean (further referred to as total swimming costs C_R (milligrams of oxygen per hour)) of the 12 or 6 V_{O_2} values obtained for each experiment.

Prior to statistical analyses, the obtained total swimming costs and body mass values were log transformed and the residuals were tested for normality using graphical probability plots. Homogeneity of variance was tested using Levene's test. Statistical analyses of total swimming cost data were performed on two groupings of our experiments. The first grouping (further referred to as G1) comprised 96 experiments (8 fish masses × 3 water temperatures × 4 flow conditions). G1 allowed us to test the variability of total swimming costs with water temperature, mean flow velocity (18 and 23 $cm \cdot s^{-1}$), and standard deviation of flow velocity (5 and 8 $cm \cdot s^{-1}$) using a three-way ANOVA. During this analysis, fish body mass was used as a covariate. The second grouping (further referred to as G2) consisted of 40 experiments performed at 15 °C using eight fish masses and five flow conditions (mean flow of 18 and 23 $cm \cdot s^{-1}$ and standard deviation of 5 and 8 $cm \cdot s^{-1}$ together with mean flow of 40 $cm \cdot s^{-1}$ and standard deviation of 10 $cm \cdot s^{-1}$). G2 was used to test the significance of the effect of mean flow and standard deviation of flow on total swimming costs over a wider range of flow turbulence than with G1 but at a single water temperature. This analysis was performed with a two-way ANOVA using fish mass as a covariate.

The relationship between total swimming costs and body mass, water temperature (only for G1), and flow characteristics was assessed using multiple regression analyses. Three different types of models were explored. These models were defined by the variable(s) used to represent flow. Following this procedure, flow characteristics were alternately represented by (*i*) the mean and the standard deviation of flow velocity, (*ii*) the turbulence intensity, and (*iii*) the turbulent kinetic energy.

Results

Total swimming costs

The oxygen depletion in the respirometer was linear over time during all experiments ($0.89 < r^2 < 1.0$, $p < 0.001$). Consequently, no relationship between oxygen consumption rates C_R and time since the beginning of an experiment was observed ($0.01 < r^2 < 0.13$, $0.24 < p < 1.0$) (Fig. 1). Within-experiment variation in C_R ranged from 3.8% to 11.6%. The total swimming costs varied 9.3-fold among our experiments (1.6–14.9 mg $O_2 \cdot h^{-1}$) (Table 2). Data comprised in our first grouping of experiments (G1) indicated that total swimming costs increased twofold as fish mass increased from 5 to 15 g. As expected, total swimming costs increased with water temperature (Fig. 2). For instance, depending on the flow conditions, the total swimming costs of a 10-g fish increased by 10.5%–16.9% as water temperature increased from 10 to 20 °C. Total swimming costs also tended to increase with mean flow velocity and with the standard deviation of flow velocity (Fig. 3). Hence, the total swimming costs of a 10-g fish increased, on average, by 61.4% as mean flow velocity

Fig. 1. Oxygen consumption rates during the experimental period of four juvenile Atlantic salmon (*Salmo salar*): a 5.3-g fish at 10 °C, $\bar{u}$ = 18 cm·s^{-1}, and u_{SD} = 5 cm·s^{-1} (solid circles); a 9.6-g fish at 15 °C, $\bar{u}$ = 23 cm·s^{-1}, and u_{SD} = 5 cm·s^{-1} (open circles); a 15.0-g fish at 20 °C, $\bar{u}$ = 23 cm·s^{-1}, u_{SD} = 8 cm·s^{-1} (solid triangles); and a 11.6-g fish at 15 °C, $\bar{u}$ = 40 cm·s^{-1}, and u_{SD} = 10 cm·s^{-1} (open triangles). Regression lines of the linear relationship between time and oxygen consumption rates are presented.

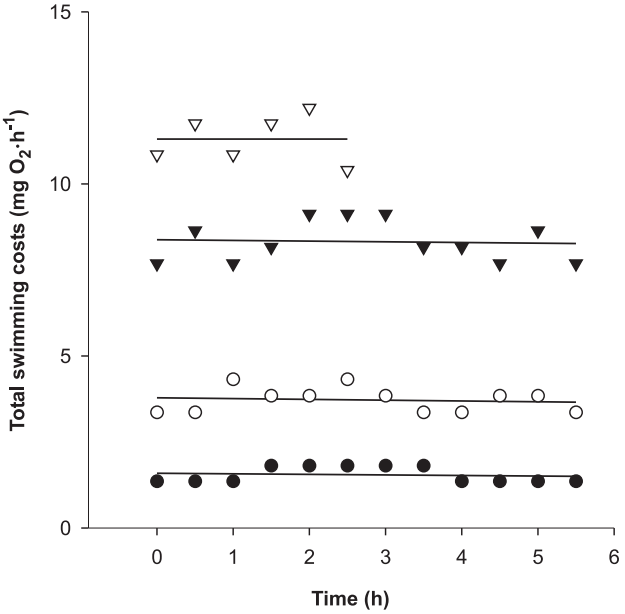

increased from 18 to 23 cm·s^{-1}, while standard deviation was constant at 5 cm·s^{-1}. The corresponding increase of total swimming costs with a standard deviation of flow of 8 cm·s^{-1} was 52.9%. On average, total swimming costs of a 10-g fish increased by 31.9% ($\bar{u}$ = 18 cm·s^{-1}) and by 25.0% ($\bar{u}$ = 23 cm·s^{-1}) as the standard deviation of the flow velocity increased from 5 to 8 cm·s^{-1}.

Swimming costs model

Statistical analyses indicated that body mass ($F_{[1,83]}$ = 447.16, $p < 0.001$), water temperature ($F_{[2,83]}$ = 17.55, $p < 0.001$), mean flow velocity ($F_{[1,83]}$ = 650.62, $p < 0.001$), and standard deviation of flow velocity ($F_{[1,83]}$ = 196.05, $p < 0.001$) had a significant effect on total swimming costs. No interaction term of the three-way ANOVA was significant ($0.10 < p < 0.99$), indicating that the direction of the effect of body mass, water temperature, mean flow velocity, and standard deviation of flow velocity on the total swimming costs was similar among the different combinations of experimental conditions. Body mass, water temperature, and mean and standard deviation of flow velocity explained a statistically significant proportion of the variations of total swimming costs ($F_{[4,91]}$ = 337.37, R^2 = 0.93, $p < 0.001$) (Table 3). Mean flow velocity and body mass explained respectively 46% and 31% of the variations of total swimming costs, while standard deviation of flow velocity explained 14% of this variation. Water temperature explained 2% of the observed variations of total swimming costs. Total swimming costs could not be related to turbulence intensity. In contrast, a model combining body mass, water temperature, and turbulent kinetic energy explained 49% of the variation in total swimming costs ($F_{[3,92]}$ = 29.41, $p < 0.001$). The most influential variable in this model was the body mass, which explained 31% of the variance of total swimming costs. Turbulent kinetic energy and water temperature explained respectively 16% and 3% of the variations of total swimming costs.

Table 2. Temperature, flow condition (selected combination of mean flow velocity ($\bar{u}$) and standard deviation of flow velocity (u_{SD})), range of body mass (M) of fish used in the respirometry experiments, and total swimming costs (C_R) measured in the corresponding turbulence flow condition.

Temperature (°C)	$\bar{u}$ (cm·s^{-1})	u_{SD} (cm·s^{-1})	M (g wet mass)	C_R (mg O_2·h^{-1})
10	18	5	5.3–16.4	1.5–3.2
	18	8	5.6–16.3	1.7–4.1
	23	5	5.4–17.6	2.2–5.5
	23	8	6.4–15.0	3.5–7.1
15	18	5	5.6–15.5	1.6–3.5
	18	8	5.2–15.0	2.0–4.3
	23	5	4.9–16.0	2.7–6.0
	23	8	5.1–15.0	3.7–8.0
	40	10	4.3–14.0	5.0–14.9
20	18	5	5.2–15.2	1.7–3.9
	18	8	5.9–16.1	2.4–5.1
	23	5	5.9–16.1	2.7–6.2
	23	8	5.9–16.8	3.6–8.2

Note: Number of experiments (n) equalled 8 for each combination of water temperature and flow condition.

Data included in our second grouping of experiments (G2) confirmed the effects of body mass on the total swimming costs. The observations performed at higher mean flow velocities indicated that body mass ($F_{[1,34]}$ = 285.87, $p < 0.001$), mean flow velocity ($F_{[1,34]}$ = 294.27, $p < 0.001$), and standard deviation of flow velocity ($F_{[1,34]}$ = 83.46, $p < 0.001$) significantly affected total swimming costs. The interaction term between mean and standard deviation of flow velocity was not significant (p = 0.71), indicating that the direction of the effect of two variables on the total swimming costs was similar among the different experimental conditions. Multiple regression analyses based on G2 allowed us to develop a three-variable model ($F_{[3,36]}$ = 146.30, R^2 = 0.92, $p < 0.001$) where body mass, mean flow velocity, and standard deviation of flow velocity contributed respectively to 16%, 61%, and 15% of the variation in total swimming costs. We again observed no correlation between the turbulence intensity and the total swimming costs. However, total swimming costs increased with body mass and turbulent kinetic energy, resulting in a two-variable model ($F_{[2,37]}$ = 53.46, R^2 = 0.74, $p < 0.001$) with body mass contributing 16% and turbulent kinetic energy 58% of the variation in total swimming costs.

Discussion

Our analyses demonstrated that total swimming costs of JAS swimming in turbulent flow increased with body mass, water temperature, mean flow velocity, standard deviation of flow velocity, and turbulent kinetic energy. The exponent of

Fig. 2. Total swimming costs of juvenile Atlantic salmon (*Salmo salar*) at four different flow conditions: (*a*) $\bar{u}$ = 18 cm·s^{-1} and u_{SD} = 5 cm·s^{-1}, (*b*) $\bar{u}$ = 18 cm·s^{-1} and u_{SD} = 8 cm·s^{-1}, (*c*) $\bar{u}$ = 23 cm·s^{-1} and u_{SD} = 5 cm·s^{-1}, and (*d*) $\bar{u}$ = 23 cm·s^{-1} and u_{SD} = 8 cm·s^{-1} at 10 °C (triangles), 15 °C (open circles), and 20 °C (solid circles). Values are means ± SE (n = 12). Regression lines of the log linear relationship between body mass and total swimming costs are presented.

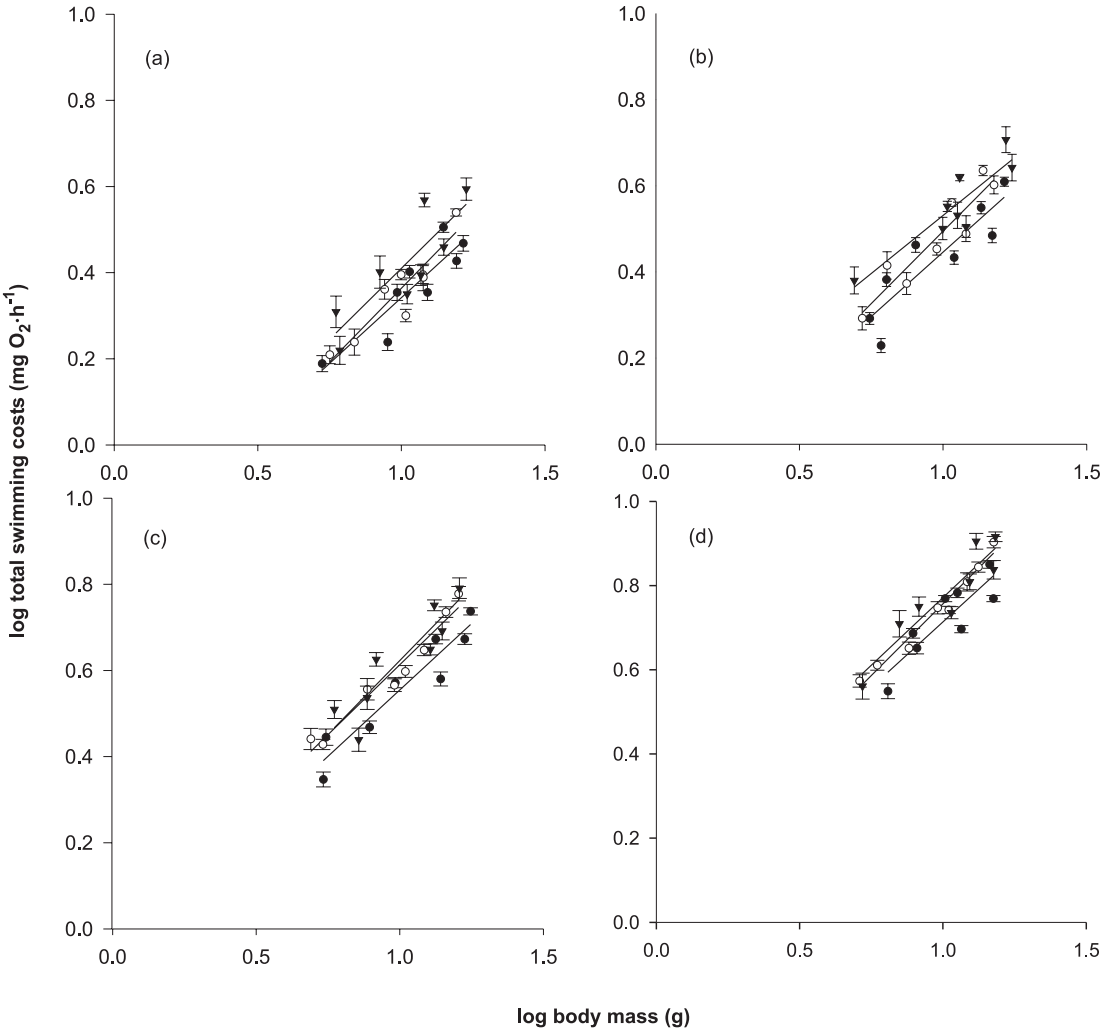

body mass (0.62–0.79 depending on the model) was similar to those of models developed for forced-swimming models, indicating that the slope of the increase of metabolic rates of fish was similar to that found in other swimming costs models. Our analyses suggest that water temperature explained a significant proportion of the variations in the metabolic rates. A 10 °C increase in water temperature increased total respiration rates by 12%–18%. It has long been recognized that fish swimming costs increase with swimming velocity (Beamish 1978; Boisclair and Tang 1993; Tang et al. 2000). Our study confirmed this situation but also indicated that descriptors of flow turbulence explain a significant fraction of total swimming costs. The energetic costs of swimming at a given mean flow velocity increased by 21%–31% as the standard deviation of the flow velocity increased from 5 to 8 cm·s^{-1}. Among the three descriptors of flow turbulence that we examined, standard deviation of flow velocity and turbulent kinetic energy significantly contributed to the predictive power of the models developed. In contrast, turbulence intensity never explained a significant fraction of the variation of the total swimming costs. Standard deviation of flow velocity explained from 14% (with G1) to 15% (with G2) of the variations of total swimming costs compared with 16% (with G1) to 58% (with G2) for turbulent kinetic energy. Hence, turbulent kinetic energy appears to be a more powerful predictor of total swimming costs than standard deviation of low flow velocity alone. However, the combination of mean flow velocity and standard deviation of flow velocity explained a higher fraction of the variations of total swimming costs (from 60% to 76%) than turbulent kinetic energy. This suggests that the model using mean and standard deviation of flow velocity may have the highest predictive power.

Comparison between observed swimming costs and predictions by forced-swimming models

Most studies that estimate the cost of swimming for stream-dwelling fish use respiration models based on experimental designs that minimize flow heterogeneity (Brett 1964; Beamish 1978). Our findings suggest that flow turbulence significantly increases fish swimming costs and consequently that the use of such forced-swimming models may

Fig. 3. Total swimming costs of juvenile Atlantic salmon (*Salmo salar*) under low (triangles), medium (circles), and high (squares) flow velocities at water temperatures of (*a*) 10 °C, (*b*) 15 °C, and (*c*) 20 °C. The open symbols represent the low turbulence condition and the solid symbols represent the medium and the high turbulence conditions. Values are means ± SE (n = 12 for the low and medium flow velocities and n = 6 for the high flow velocity). Regression lines of the log linear relationship between body mass and total swimming costs are presented.

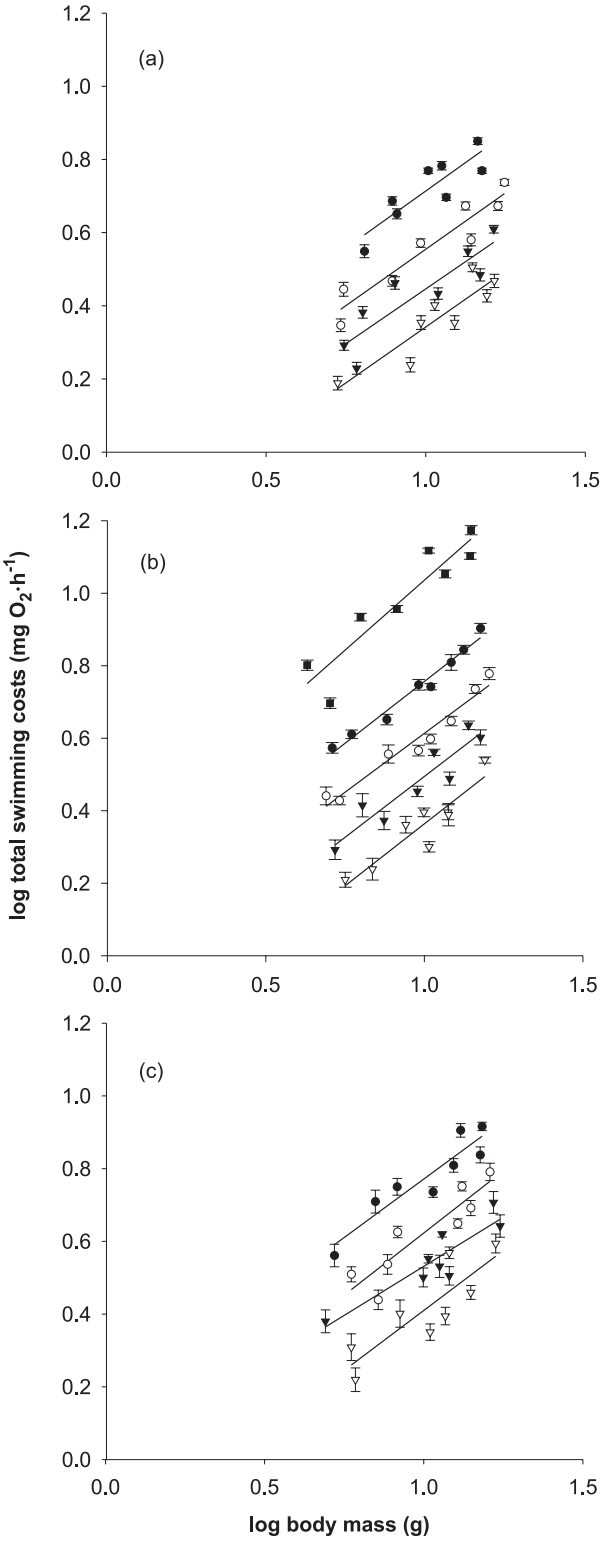

underestimate actual swimming costs. This situation can be illustrated by comparing the predictions of our turbulence swimming model with predictions of a classical forced-swimming model proposed by Boisclair and Tang (1993). However, this forced-swimming model predicts the net swimming costs of fish. In contrast, our observations and models focused on total swimming costs (standard metabolic rate plus net swimming costs). This strategy was used in the absence of a standard metabolic rate model for JAS compromising the entire body mass and water temperature ranges used in our study. Consequently, to perform the comparison between the models, we reanalysed the data set used by Boisclair and Tang (1993) and developed a new forced-swimming model predicting total swimming costs. The forced-swimming model we obtained is

$$\log_{10}\mathrm{FTSC} = 0.96\log_{10}M + 0.23\log_{10}\bar{u} + 0.67\log_{10}T - 1.85 \quad (3)$$

where FTSC is the forced total swimming costs (milligrams of oxygen per hour) under minimized flow heterogeneity, M is the fish body mass (grams wet), T is the water temperature (degrees Celsius), and $\bar{u}$ is the mean flow velocity (centimetres per second). All variables were significant; however, body mass explained most (79%) of the variation in the total swimming costs ($F_{[3,114]}$ = 162.35, R^2 = 0.81, $p < 0.0001$). The model predicted that total swimming costs of a 10-g fish swimming in minimized flow heterogeneity at a water temperature of 15 °C and a swimming speed of 18 and 23 cm·s^{-1} should be 1.50 and 1.58 mg O_2·h^{-1}, respectively. Under low-turbulence conditions, the total swimming costs that we estimated for 10-g JAS at 15 °C were 2.0 to 2.7 times higher than predicted by the forced-swimming model (Fig. 4). The differences were more pronounced under medium-turbulence conditions, ranging from 3.0- to 3.6-fold. Under high-turbulence conditions, we observed a further increase in the difference between our estimation and prediction of the forced-swimming model. The estimated total swimming costs were 14.0 times higher than predicted by the forced-swimming model. However, it is important to note that this comparison should only be taken as an indication because we extrapolate the prediction of the forced-swimming model to a twofold higher flow velocity than the model was originally developed to (maximal flow velocity 20 cm·s^{-1}).

The increase in the actual total swimming costs under turbulent conditions above those predicted by the forced-swimming model is consistent with the hypothesis that unsteady swimming movements, such as active accelerations and decelerations and changes in speed, are energetically more costly than steady swimming movements at constant speed and direction (Webb 1983; Boisclair and Tang 1993; Kramer and McLaughlin 2001). In turbulent flow, fish have to adjust to the fluctuations in velocity and direction of flow by constantly moving their fins to maintain their position. These movements substantially increase the energetic costs of unsteady swimming above those of steady swimming for the same average swimming speed (Tang et al. 2000; Enders and Herrmann 2003).

The experimental flow conditions used in our experiments are within the range of mean flow velocities (5–40 cm·s^{-1}) (DeGraaf and Bain 1986; Guay et al. 2000) and of standard deviations of flow velocity (4–14 cm·s^{-1}) JAS experience at

Table 3. Four multiple regression models to estimate the total swimming costs (C_R; mg $O_2 \cdot h^{-1}$) in turbulent flow for juvenile Atlantic salmon (*Salmo salar*) using water temperature (T), body mass (M), mean flow velocity ($\overline{u}$), standard deviation of flow velocity (u_{SD}), and turbulent kinetic energy (TKE) as explanatory variables.

	Contribution of variable					Model statistics		
Turbulent swimming model	T (°C)	M (g wet mass)	$\overline{u}$ (cm·s^{-1})	u_{SD} (cm)	TKE (g·cm^{-1}·s^{-2})	n	R^2	p
$\log C_R = 0.23 \log T + 0.64 \log M + 2.43 \log \overline{u} + 0.67 \log u_{SD} - 4.06$	0.02	0.31	0.46	0.14	0.16	96	0.93	<0.001
$\log C_R = 0.23 \log T + 0.62 \log M + 0.44 \log \mathrm{TKE} - 1.21$	0.03	0.31				96	0.49	<0.001
At 15 °C								
$\log C_R = 0.79 \log M + 1.47 \log \overline{u} + 0.47 \log u_{SD} - 2.45$		0.16	0.61	0.15		40	0.92	<0.001
$\log C_R = 0.66 \log M + 0.68 \log \mathrm{TKE} - 1.44$		0.16			0.58	40	0.74	<0.001

Fig 4. Ratios of the total swimming costs in turbulent and forced swimming for different fish body mass and flow conditions at (*a*) 10 °C and (*b*) 20 °C. Light and dark lines represent the flow conditions with mean flow velocity $\overline{u}$ of 18 cm·s^{-1} and 23 cm·s^{-1}, respectively. Broken lines indicate low turbulence condition u_{SD} of 5 cm·s^{-1}, and solid lines indicate medium turbulence conditions of 8 cm·s^{-1}.

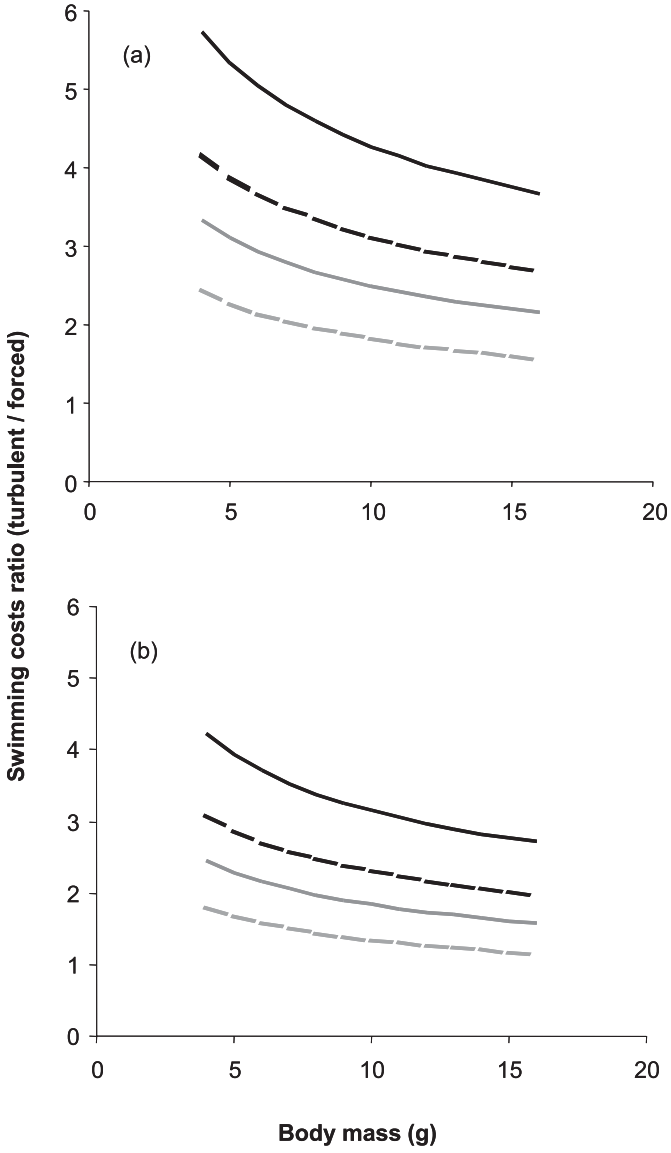

their station-holding position in nature. At their station-holding position, JAS also experience intense flow velocity fluctuations often referred to as large-scale flow structures. These large-scale flow structures are intermittent fluids of high velocity divided by fluids of low velocity. We simulated these large-scale flow structures in our respirometer. The examination of the velocity time series allowed us to identify from two to five low-speed flow events per minute and five high-speed flow events per minute. The mean duration of the flow events was 1.0 s (SD = 0.24 s). However, in their natural environment, JAS are also exposed to a variety of spatial flow structures such as vortices, which are generated by the roughness of the riverbed. Protruding obstacles like the

"home rocks" of JAS used as station-holding positions during active foraging cause the formation of vortex shedding motions at the lee side of obstacles. Liao et al. (2003) demonstrated in a laboratory study that adult rainbow trout might profit from the energy of such vortex shedding. Fish changed their swimming patterns to slalom between the vortices resulting in a reduction of the axial muscle activity. Similarly, it has been suggested that adult sockeye salmon (*Oncorhynchus nerka*) exploit recirculation zones during upriver spawning migration to minimize the energy expenditures (Hinch and Rand 1998; Standen et al. 2002). It is also known that schooling fish profit from the vortices generated by the leading fish. Sea bass (*Dicentrarchus labrax*) swimming at speed of 15–32 $cm \cdot s^{-1}$ in front of the fish school had a 9%–14% higher tail beat frequency than the fish swimming in the rear (Herskin and Steffensen 1998). This behavior resulted in a decrease of the total swimming costs of 9%–23%. The studies demonstrate that under stable vortex shedding, fish may use the energy of these vortices to minimize their energy expenditure of swimming. However, in their natural flow environments, vortex shedding is quasi-periodic phenomena and therefore less regular than simulated in laboratory studies (Roy et al. 1999). This means that under natural flow conditions, fish experience vortex shedding that is less predictable than under laboratory conditions. Therefore, it may be more difficult for fish in natural flow environments to benefit from vortex shedding than demonstrated in laboratory studies.

The applicability of the turbulent swimming model to field situations depends on the ability of our experimental design to reflect natural conditions found in rivers and streams and on the validity of the assumptions that we used to estimate fish swimming costs. First, the model is based on the assumption that the experimental conditions allow fish to swim in a way that may mimic their swimming in the field. Therefore, we tried in swimming experiments to simulate natural flow conditions choosing mean and standard deviation of flow velocities as well as pulses of high- and low-speed flow velocities as observed under natural conditions. However, it is well understood that our results do not cover the complete range of flow conditions that JAS may encounter in natural environments.

Second, the model assumes that, within the range of the duration of the experiments performed, the length of an experiment (hours) has no effect on the validity of the respiration rates obtained. The swimming experiments may be particularly susceptible to this assumption because the experiments required that fish swim continuously for hours at steady swimming speeds, which may not correspond to the natural behavior of JAS. The approach also assumes that, if fish continue to swim for the complete duration of an experiment, and if the metabolic rates do not significantly increase or decrease through time, fish are not fatigued and that their metabolic rates adequately represent swimming costs under the experimental conditions. As such, when developing swimming costs models, combinations of swimming intensity and duration of the experiments are selected to avoid fatigue. In our experiments, the metabolic rate was independent of time, indicating that time spent swimming had no effect on the models developed within the swimming durations used in our study.

Third, the model assumes that swimming costs are adequately estimated by measuring oxygen consumption by fish. This assumption also presumes that the energy required to swim comes mostly from the aerobic metabolism. If anaerobic metabolism contributes to the swimming costs, the potential exists for oxygen consumption rates to underestimate actual swimming costs. The anaerobic metabolism could theoretically interfere with estimates of fish swimming costs obtained by measuring oxygen consumption by fish. The interference caused by anaerobic metabolism is circumvented by modulating the experimental flow velocities and the duration of the experiments to minimize the expression of anaerobic metabolism.

Fourth, the model is based on the assumption that the 2-day deprivation period permitted, on one hand, the exclusion of any increased oxygen consumption rates due to digestion and, on the other hand, did not affect the swimming performance of the fish due to depletion of muscle metabolites (Beamish 1964).

Fifth, we assume that body size rather than fish age influences the swimming performance of fish. The fish that we used for the respirometry experiments were all from the same cohort (age 1+ at the beginning of the experimental period and age 2+ at the end). However, no data are available to determine to what extent fish age actually influences the swimming performance.

The models of total swimming costs in turbulent flow that we developed may be applied to estimate the energy expenditures that JAS would experience in situations where they swim in turbulent flow. These situations may include foraging attempts in the water column to capture drifting food particles or migrations between different habitats (e.g., changes between summer and winter habitat). The models may also be applied to nonterritorial individuals that inhabit the spaces between territories (Martel 1996). The foraging strategy of nonterritorial individuals differs from the commonly described station-holding behavior of JAS. The nonterritorial fish may minimize their energy expenditure related to territorial defense, but they may do so at the expense of increased swimming costs due to exposure to turbulent flow. It is anticipated that in situations where territorial JAS use home rocks in their typical sit-and-wait position near the substrate, no increase in the metabolic costs due to activity occurs (Facey and Grossman 1990). Similarly, in situations where JAS seek shelter in the interstices of the riverbed substrate, especially during low water temperature, no increase in the swimming costs are anticipated (Cunjak 1988; Bremset 2000).

This study showed that bioenergetics models aiming to estimate the energetic costs of habitat utilization by stream-dwelling fish in turbulent environments may require both a description of the behavior of the fish in relation to turbulence and swimming costs models in which the effects of the flow turbulence are explicitly represented. The comprehension of the effects of turbulence on swimming costs may also be relevant to models developed for habitat restoration and management and to the design of migratory fish passages (Odeh et al. 2002; Guiny et al. 2003). We conclude that turbulent swimming models using the mean and standard deviation of flow velocity or turbulent kinetic energy may provide estimates of the cost of habitat utilization for

stream-dwelling fish that are more accurate than the commonly used forced-swimming models.

Acknowledgements

We thank the Pisciculture de Tadoussac for providing us the juvenile Atlantic salmon, Jean-Pierre Martin and Guillaume Guénard for their help in constructing the turbulence-creating transformer, and Judith Bouchard and Sébastien Dupuis for their help in fish husbandry and during the respirometry experiments. Normand Bergeron graciously provided the acoustic Doppler velocimeter. Funding for this study was provided by an individual grant from the Natural Sciences and Engineering Research Council of Canada and by Fonds pour les Chercheurs et l'Aide à la Recherche (FCAR-Équipe) to D. Boisclair. E.C. Enders was supported by scholarships from the Fondation Joseph-Arthur Paulhus, the Faculté des Études Supérieures (Université de Montréal), and the Groupe de Recherche Interuniversitaire en Limnologie (GRIL, FCAR-Centre).

References

Beamish F.W.H. 1964. Respiration of fishes with special emphasis on standard oxygen consumption. II. Influence of weight and temperature on respiration of several species. Can. J. Zool. **42**: 177–188.

Beamish, F.W.H. 1978. Swimming capacity. *In* Fish physiology — locomotion. *Edited by* W.S. Hoar and J.R. Randall. Academic Press, New York. pp. 101–187.

Boisclair, D., and Leggett, W.C. 1989. The importance of activity in bioenergetics models applied to actively foraging fishes. Can. J. Fish. Aquat. Sci. **46**: 1859–1867.

Boisclair, D., and Tang, M. 1993. Empirical analysis of the influence of swimming pattern on the net energetic cost of swimming in fishes. J. Fish Biol. **42**: 169–183.

Bremset, G. 2000. Seasonal and diel changes in behaviour, microhabitat use and preferences by young pool-dwelling Atlantic salmon, *Salmo salar*, and brown trout, *Salmo trutta*. Environ. Biol. Fishes, **59**: 163–179.

Brett, J.R. 1964. The respiratory metabolism and swimming performance of young sockeye salmon. J. Fish. Res. Board Can. **21**: 1183–1226.

Brett, J.R., and Groves, D.D. 1979. Physiological energetics. *In* Fish physiology — bioenergetics and growth. *Edited by* W.S. Hoar, J.R. Randall, and J.R. Brett. Academic Press, New York. pp. 279–352.

Cunjak, R.J. 1988. Behaviour and microhabitat of young Atlantic salmon (*Salmo salar*) during winter. Can. J. Fish. Aquat. Sci. **45**: 2156–2160.

Cunjak, R.A., and Therrien, J. 1998. Inter-stage survival of wild juvenile Atlantic salmon, *Salmo salar* L. Fish. Manag. Ecol. **5**: 209–223.

Cutts, C.J., Metcalfe, N.B., and Taylor, A.C. 1998. Aggression and growth depression in juvenile Atlantic salmon — the consequences of individual variation in standard metabolic rate. J. Fish Biol. **52**: 1026–1037.

DeGraaf, D.A., and Bain, L.H. 1986. Habitat use by and preferences of juvenile Atlantic salmon in two Newfoundland rivers. Trans. Am. Fish. Soc. **115**: 671–681.

Enders, E.C., and Herrmann, J.P. 2003. Energetic costs of spontaneous activity in horse mackerel quantified by a computerized imaging analysis. Arch. Fish. Mar. Res. **50**: 205–219.

Enders, E.C., Boisclair, D., and Roy, A.G. 2003. The effect of turbulence on the cost of swimming for juvenile Atlantic salmon (*Salmo salar*). Can. J. Fish. Aquat. Sci. **60**: 1149–1160.

Enders, E.C., Buffin-Bélanger, T., Boisclair, D., and Roy, A.G. 2005. The feeding behaviour of juvenile Atlantic salmon in relation to turbulent flow. J. Fish Biol. **66**: 242–253.

Facey, D.E., and Grossman, G.D. 1990. The metabolic cost of maintaining position for four North American stream fishes: effects of season and velocity. Physiol. Zool. **63**: 757–776.

Fausch, K.D. 1984. Profitable stream positions for salmonids: relating specific growth rate to net energy gain. Can. J. Zool. **62**: 441–451.

Guay, J.C., Boisclair, D., Rioux, D., Leclerc, M., Lapointe, M., and Legendre, P. 2000. Development and validation of numerical habitat models for juveniles of Atlantic salmon (*Salmo salar*). Can. J. Fish. Aquat. Sci. **57**: 2065–2075.

Guiny, E., Armstrong, J.D., and Ervine, D.A. 2003. Preferences of mature male brown trout and Atlantic salmon parr for orifice and weir fish pass entrances matched for peak velocities and turbulence. Ecol. Freshw. Fish, **12**: 190–195.

Hansen, M.J., Boisclair, D., Brandt, S.B., Hewett, S.W., Kitchell, J.F., Lucas, M.C., and Ney, J.J. 1993. Applications of bioenergetics models to fish ecology and management — where do we go from here? Trans. Am. Fish. Soc. **122**: 1019–1030.

Herskin, J., and Steffensen, J.F. 1998. Energy savings in sea bass swimming in a school — measurements of tail beat frequency and oxygen consumption at different swimming speeds. J. Fish Biol. **53**: 366–376.

Hill, J., and Grossman, G.D. 1993. An energetic model of microhabitat use for rainbow trout and rosyside dace. Ecology, **74**: 685–698.

Hinch, S.G., and Rand, P.S. 1998. Swim speeds and energy use of upriver-migrating sockeye salmon (*Oncorhynchus nerka*) — role of local environment and fish characteristics. Can. J. Fish. Aquat. Sci. **55**: 1821–1831.

Hutchings, J.A., and Jones, M.E.B. 1998. Life history variation and growth rate thresholds for maturity in Atlantic salmon, *Salmo salar*. Can. J. Fish. Aquat. Sci. **55**: 22–47.

Kalleberg, H. 1958. Observations in a stream tank of territoriality and competition in juvenile Atlantic salmon and trout (*Salmo salar* L. and *S. trutta* L.). Fish. Board Swed. Inst. Freshw. Res. Drottingholm Rep. **39**: 55–98.

Kramer, D.L., and McLaughlin, R.L. 2001. The behavioral ecology of intermittent locomotion. Am. Zool. **41**: 137–153.

Liao, J.C., Beal, D.N., Lauder, G.V., and Triantafyllou, M.S. 2003. Fish exploiting vortices decrease muscle activity. Science (Wash., D.C.), **302**: 1566–1569.

Martel, G. 1996. Growth rate and influence of predation risk on territoriality in juvenile coho salmon (*Oncorhynchus kisutch*). Can. J. Fish. Aquat. Sci. **53**: 660–669.

Morgan, I.J., McCarthy, I.D., and Metcalfe, N.B. 2000. Life-history strategies and protein metabolism in overwintering juvenile Atlantic salmon: growth is enhanced in early migrants through lower protein turnover. J. Fish Biol. **56**: 637–647.

Morgan, I.J., McCarthy, I.D., and Metcalfe, N.B. 2002. The influence of life-history strategy on lipid metabolism in overwintering juvenile Atlantic salmon. J. Fish Biol. **60**: 674–686.

Ney, J.F. 1993. Bioenergetics modelling today: growing pains on the cutting edge. Trans. Am. Fish. Soc. **122**: 736–748.

Nislow, K.H., Folt, C.L., and Parrish, D.L. 2000. Spatially explicit bioenergetic analysis of habitat quality for age-0 Atlantic salmon. Trans. Am. Fish. Soc. **129**: 1067–1081.

Odeh, M., Noreika, J.F., Haro, A., Maynard, A., Castro-Santos, T., and Cada, G.F. 2002. Evaluation of the effects of turbulence on

the behavior of migratory fish. Final report 2002. Report to Bonneville Power Administration, Contract No. 00000022, Project No. 200005700 (BPA Report DOE/BP-00000022-1). Available at www.efw.bpa.gov/Publications/D00000022-1.pdf.

Pavlov, D.S., Lupandin, A.I., and Skorobogatov, M.A. 2000. The effects of flow turbulence on the behavior and distribution of fish. J. Ichthyol. **40**: S232–S261.

Roy, A.G., and Buffin-Bélanger, T. 2001. Advances in the study of turbulent flow structures in gravel-bed rivers. *In* Gravel-bed river. V. *Edited by* M.P. Mosley. New Zealand Hydrological Society, Christchurch, New Zealand. pp. 375–397.

Roy, A.G., Biron, P.M., Buffin-Bélanger, T., and Levasseur, M. 1999. Combined visual and quantitative techniques in the study of natural turbulent flows. Water Resour. Res. **35**: 871–877.

Roy, A.G., Buffin-Bélanger, T., Lamarre, H., and Kirkbride, A.D. 2004. Size, shape and dynamics of large-scale turbulent flow structures in a gravel-bed river. Water Resour. Res. **500**: 1–27.

Standen, E.M., Hinch, S.G., Healey, M.C., and Farrell, A.P. 2002. Energetic costs of migration through the Fraser River Canyon, British Columbia, in adult pink (*Oncorhyncus gorbuscha*) and sockeye (*Oncorhynchus nerka*) salmon as assessed by EMG telemetry. Can. J. Fish. Aquat. Sci. **59**: 1809–1818.

Tang, M., Boisclair, D., Menard, C., and Downing, J.A. 2000. Influence of body weight, swimming characteristics, and water temperature on the cost of swimming in brook trout (*Salvelinus fontinalis*). Can. J. Fish. Aquat. Sci. **57**: 1482–1488.

Webb, P.W. 1983. Speed, acceleration and manoeuvrability of two teleost fishes. J. Exp. Biol. **102**: 115–122.